J Solid State Electrochem (2012) 16:1663–1673
DOI 10.1007/s10008-011-1579-1

ORIGINAL PAPER

The effects of pretreatment of polycrystalline gold with $OH^{\bullet}$ radicals on the electrochemical nucleation and growth of platinum

Gustav Sievers · Ulrich Hasse · Fritz Scholz

Received: 15 July 2011 / Revised: 3 August 2011 / Accepted: 16 October 2011 / Published online: 6 November 2011

Abstract The nucleation and growth of platinum on polycrystalline gold was studied by chronoamperometry, cyclic voltammetry, and atomic force microscopy before and after treatment of the gold surface with hydroxyl ($OH^{\bullet}$) radicals. Two different procedures of mechanical polishing of the gold surface ("coarse polish" and "fine polish") were applied before the treatment with $OH^{\bullet}$ radicals. The nucleation and growth of Pt was much better reproducible on electrodes which underwent a "coarse polish". The treatment of the Au surface with $OH^{\bullet}$ radicals decreased the number of active sites; however, the nucleation growth mode remained the same (3-D instantaneous). The spontaneous Pt deposition (no externally applied potential) on Au was unaffected by the treatment with $OH^{\bullet}$ radicals. In situ atomic force microscopy experiments showed that the Pt starts to grow only on some of the Au grains, most probably on those which have active sites on their surface. This leads to a roughening of the electrode surface upon Pt deposition. Treatment with $OH^{\bullet}$ radicals did only quantitatively diminish the amount of deposited Pt, but qualitatively the imaging of the Pt growth remained the same. Obviously, the $OH^{\bullet}$ radicals lead to a knockout (decreasing number) of active sites for Pt nucleation, while the nature of the remaining active sites stays unaffected.

Keywords Electrochemistry · Nucleation and growth · Hydroxyl radical · Active center · Nucleation sites · Gold · Platinum

G. Sievers · U. Hasse · F. Scholz (✉)
Institut für Biochemie, Universität Greifswald,
Felix-Hausdorff-Straße 4,
17487 Greifswald, Germany
e-mail: fscholz@uni-greifswald.de

Introduction

The elucidation of the nature of active centers on surfaces is one of the most demanding tasks in catalysis and generally in surface science. When using the term "active center" one always has to specify what activity is meant. On a surface there can be active centers for the catalysis of certain chemical reactions, e.g., of oxidations or reductions, for the formation of gas bubbles when the surface is in contact with a supersaturated gas solution, for the precipitation of crystals when the surface is in contact with a supersaturated salt solution, for the growth of an oxide or for the pit formation by corrosive dissolution, for the electrochemical deposition of a foreign metal when the surface is in contact with a supersaturated metal solution etc., and all these active centers may differ in nature.

The identification and manipulation of "active centers" is crucial in heterogeneous catalysis [1] where the behavior of nanometer down to atomic sized centers can be of immense importance for the development. In 1925, Taylor introduced [2] the idea of active centers as defect sites; a view which has been supported by many experimental results [1, 3, 4]. However, the various structures and mechanisms of action of all different kinds of active centers are still a hot topic, not only in catalysis, but also in corrosion, plating, and generally when phase transitions play a role. It is well-known that variations of the electronic structure and geometry are frequently determining parameters [5].

In order to obtain a better understanding of the nature of active sites, we have recently started to apply the following approach: The surface of an electrode is treated with hydroxyl ($OH^{\bullet}$) radicals and the effect of that treatment on the electrochemical and the electrocatalytic behavior of the electrode is monitored, as well as the surface is characterized

by spectroscopic and microscopic techniques [6–9]. The main results of these studies can be summarized as follows: (1) treatment of the highly electrocatalytically active metals Pt (polycrystalline Pt=*pc*–Pt) and Pd (polycrystalline Pd=*pc*–Pd) with $OH^{\bullet}$ radicals do not, or only marginally, affect their electrochemical and electrocatalytic properties. (2) However, the electrocatalytic activity of the less active metals Ag (polycrystalline Ag=*pc*–Ag) and Au (polycrystalline Au=*pc*–Au) are seriously affected. In the case of *pc*–Au and *pc*–Ag, the surface asperities are also the locus of the catalytically active sites which means that the active sites are obviously associated *with* them and located somewhere *on* them. It seems that in case of *pc*–Pt and *pc*–Pd, the active sites are part of the regular surface structure, whereas in case of *pc*–Ag and *pc*–Au the active sites are highly reactive atoms located at places where the regular structure of the metal surface has been considerably changed by the mechanical polishing; i.e., the active sites consist of dislocated atoms which may be more easily oxidized (or rehybridized in the sense of d→s). Ag and Au, due to their electronic structure, will attain a d^{10-x} electron configuration, a state which can be stabilized at such locations. The d^{10-x} with $x=1$ electron configuration is exactly that which is made responsible for the electrocatalytic activity of regular surface atoms of Pt, and probably also of catalytically active Pd atoms [10]. In this connection, it is interesting that in case of gold deposited on titania, it has been shown that for CO oxidation the most active gold consists of bilayer islands [11].

The present paper describes the results of a nucleation growth study of platinum deposition on *pc*–Au. We have selected that topic in order to see how the treatment of the gold surface with $OH^{\bullet}$ radicals will affect the nucleation growth mechanism and to compare the effects with the previously mentioned studies of electrocatalysis.

Hitherto, the deposition of platinum on gold has been the subject of numerous studies. The mechanism of electrochemical nucleation and growth of Pt from Pt(II) solutions on Au(100) and Au(111) has been found to follow the Volmer–Weber growth mode [12, 13]. The interpretation of the mechanism of electrochemical deposition of Pt from Pt (IV) solutions is inconsistent. Waibel et al. identified a Volmer–Weber growth mechanism [12] whereas Kondo et al. identified a Frank–van der Meerwe mechanism [13]. On nanoporous gold, the growth mechanism has been even identified to follow a pseudo Stranski–Krastanov mechanism [14]. Platinum is adsorbed spontaneously as Pt^{2+} and the successive reduction in platinum-free solution leads to a homogeneous nucleation and growth, not dependent on the surface morphology and the valency of platinum [15–17]. Table 1 gives a summary of previous studies of Pt deposition on Au.

Experimental section

Electrochemical instrumentation

Chronoamperometry and cyclic voltammetry were performed with an Autolab, model 302 potentiostat (Eco-Chemie, Utrecht) using a three-electrode system. A gold disk electrode (1.0 mm radius; Metrohm) was used as the working electrode, a 3 M KCl Ag/AgCl electrode ($E=0.207$ V vs. SHE at 25 °C) served as the reference electrode, and a glassy carbon rod was used as the auxiliary electrode.

Hydroxyl radical generation

The Fenton solutions had the following composition: $FeSO_4 \cdot 6H_2O$ ($c_{Fe(II)}=1\times10^{-3}$ mol L^{-1}; Merck), disodium ethylenediaminetetraacetate (Na_2EDTA; $c_{EDTA}=1\times10^{-2}$ mol L^{-1}; Merck), acetate buffer ($c_{Ac^-}=c_{HAc}=1\times10^{-1}$ mol L^{-1}; pH 4.7), and H_2O_2 ($c_{H_2O_2}=1\times10^{-2}$ mol L^{-1}). The Fenton solutions were always freshly prepared. In some experiments, the hydroxyl radicals were generated with the help of UV photolysis of H_2O_2. The UV reactor, filled with H_2O_2 solution ($c_{H_2O_2}=1\times10^{-1}$ mol L^{-1}), was used for hydroxyl radical attack before atomic force microscopy (AFM) measurements. H_2O_2 was added immediately before starting the experiments. The UV reactor was equipped with a high-pressure mercury lamp (500 W). Quartz glass vessels were used to house the H_2O_2 solution and the gold electrode.

Electrode preparation

The *pc*–Au disk electrodes have been polished following special schemes because it is not possible to chemically dissolve the precipitated Pt from the gold electrode, so that the only way of removing the Pt is mechanical abrasion and polish. However with such mechanical procedure, it can very easily happen that traces of metallic Pt remain on the *pc*–Au electrode, and these traces would of course act as nucleation centers par excellence. Therefore the following procedure was applied: (a) "Fine polish": after Pt precipitation the most upper surface layer of the electrode was removed with the help of an abrasive paper (first 63 μm, followed by 42 μm SiC; Bosch) carefully avoiding to move the electrode over areas which have been already contaminated by Pt. That abrasion was followed by polishing on 9 μm abrasive pads (3M™, 268 L Finesse-it™, part no 00127), and later using alumina powder of decreasing particle size 1.0, 0.3 μm, and finally 50 nm (Buehler) using a PSA Microcloth (Buehler). The movement of the electrode described an "8" on the polishing cloth as to assure the most even polishing. (b) "Coarse polish": same

Table 1 Conditions and growth modes of deposition of Pt on Au

Author; year	Growth mode; Volmer–Weber (VW), Frank–van der Merwe (FM), pseudo Stranski–Krastanov (SK)	Deposition mode; electrochemical deposition (ED), ultra-high vacuum (UHV)	Pt species	Au substrate
Waibel et al. [12], 2002	VW	ED	$[PtCl_6]^{2-}$	Au(111)
			$[PtCl_4]^{2-}$	Au(100)
Kondo, Uosaki et al. [13], 2010	VW FM	ED	$[PtCl_6]^{2-}$ $[PtCl_4]^{2-}$	Au(111)
Strbac et al. [15], 2007	VW (not on defects)	Spontaneous ED	$[PtCl_6]^{2-}$	Au(111)
Nagahara et al. [16], 2004	VW (not on defects)	Spontaneous ED	$[PtCl_4]^{2-}$	Au(111)
Mathur et al. [14], 2008	SK	UHV	Pt	Nanoporous gold
Matthews and Jesser [31], 1967	FM	UHV	Pt	Au(111)
Sachtler et al. [32], 1981	VW	UHV	Pt	Au(100)
Sugawara et al. [33], 1991	FM	UHV	Pt	Au(100)
Pedersen et al. [14], 1999	FM	UHV	Pt	Au(111)
Friedrich et al. [34], 1997	VW	ED	$[PtCl_6]^{2-}$	Au(111)

as in (a) but finishing with the 9 μm abrasive pads. After each polishing, the electrode was rinsed with a direct stream of water (Milli-Q, Millipore, conductivity of ca. 0.056 μS cm^{-1}), and the electrode was dried. Then the electrode was cycled between −0.3 and 1.5 V (vs. Ag/AgCl) in 0.1 M H_2SO_4 two times with a scan rate of v=50 mV s^{-1}.

Electrode exposure to Fenton solutions (treatment with hydroxyl radicals)

Following the polishing and electrochemical pretreatment, the electrode was washed with water and exposed to freshly prepared Fenton solutions for 5 min intervals. The exposure was repeated so that the overall exposure time ranged from 5 to 90 min. The reaction of the Fenton solution with the gold electrode was terminated by removing the electrode from that solution and washing it with double-distilled water.

Platinum deposition

The deposition was performed in H_2SO_4 ($c_{H_2SO_4}$ = 0.1 mol L^{-1}) solutions of commercial K_2PtCl_4 (99.99%, Sigma-Aldrich) and also using self-synthesized H_2PtCl_6. If not otherwise given, the Pt concentration was 5 mM. Before the electrochemical deposition experiments, the electrode was polarized for 60 s at E=620 mV vs. Ag/AgCl, which is slightly above the equilibrium potential. After the electrochemical deposition, the potential was set to 620 mV to stop the deposition. Before measuring the deposited amount of platinum, the gold electrode was intensively rinsed under double-distilled water and then transferred to the respective electrolyte solution.

In situ atomic force microscopy

Atomic force micrographs were recorded with a "NanoScope I" (Digital Instruments) using the software "NanoScope E 4.23r3". In situ atomic force microscopy was performed in a home-made cell (three-electrode system) where the gold disk electrode can be situated directly beneath the cantilever and the potential was controlled by an Autolab, model 101 (Eco-Chemie, Utrecht). As reference electrode, an Ag/AgCl (3 mol L^{-1} KCl) electrode was connected via a polyethylene tube filled with KCl saturated agar gel to the home-made cell. A platinum sheet was used as auxiliary electrode.

Results and discussion

Electrochemical studies

The effect of two different mechanical polishing procedures on the nucleation of Pt on pc–Au

The nucleation and growth of platinum was studied under potentiostatic conditions by applying a potential which was more negative than the potential where the deposition starts (onset potential). The standby potential was 620 mV vs. Ag/AgCl, which is slightly more positive than the equilibrium potential. The equilibrium potential is close to the Nernst potential [12]. Figure 1a shows the current transients of Pt deposition on a *pc*–Au electrode which was subjected to the so-called "coarse polish" only. The curves were recorded applying different deposition potentials. The current transients show two peaks, probably indicating a

multinuclear–multilayer growth [18] or simply a deposition on two different active sites (or active sites and "normal" Au surface atoms). The very first current peak represents the first stage of nucleation and growth of platinum on gold. The peak currents of the first cathodic peak are supposed to be proportional to the number of active centers. In Fig. 1a, the first current peak can be observed after around 4 s and the second peak after around 32 s. Increasing the overpotential shifts the maxima to shorter times, until the first peak is even merging with the initial capacitive current decay (see Fig. 1a).

The current transients depicted in Fig. 1a were in fact recorded at a later stage of the research, because the first experiments were all performed with gold electrodes which were subjected to the so-called "fine polish" (Fig. 1b) because it was expected that a meticulous polish will be the best basis for reproducible results. However, the reproducibility was much worse with the "fine polish" as can be seen from Fig. 2. That figure shows a comparison of current transients recorded with *pc*–Au electrodes after the "coarse polish" and "fine polish" but otherwise under identical conditions. These results can be understood as a sign that the "coarse polish" produces a better reproducible number and quality of active sites, whereas the "fine polish" results in a smaller number of rather different active sites from experiment-to-experiment.

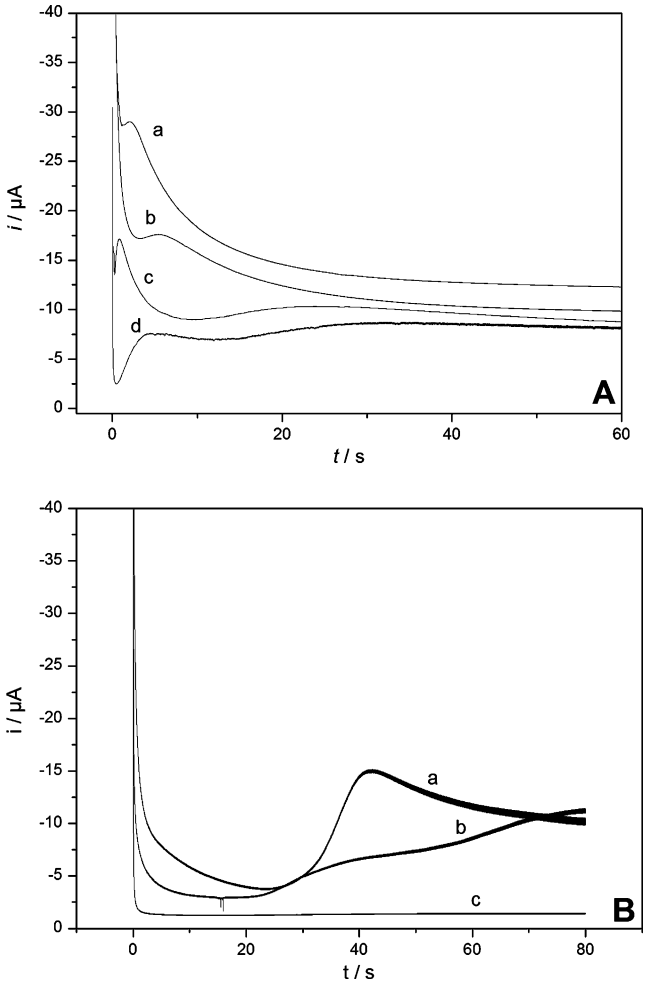

Fig. 1 Potential dependent deposition of platinum on gold. **A** Chronoamperometric deposition of Pt on *pc*–Au electrodes from solutions containing 5×10^{-3} mol L^{-1} H_2PtCl_4 and 0.1 mol L^{-1} H_2SO_4 following the "coarse polish" of the electrodes: deposition potentials E_{dep}=*a* 100 mV, *b* 200 mV, *c* 250 mV, *d* 300 mV vs. Ag/AgCl; **B** Chronoamperometric deposition of Pt on *pc*–Au electrodes from solutions composed as in **a** following the "fine polish": deposition potentials E_{dep}=*a* 150 mV, *b* 200 mV, *c* 250 mV vs Ag/AgCl

The effect of treating the pc–Au surface with hydroxyl radicals on the electrochemical nucleation of Pt on pc–Au

It has been shown earlier that $OH^{\bullet}$ radicals can effectively smooth the surface of gold [6] and selectively knockout the active centers of oxygen reduction [7]. These results encouraged us to study the effect of $OH^{\bullet}$ radicals on the active sites of Pt nucleation. We used Fenton [19] solutions for the generation of $OH^{\bullet}$ radicals. The major reaction proceeding in Fenton solutions of the used composition is the following [20]:

$$Fe^{2+} + H_2O_2 \rightarrow OH^{\bullet} + OH^{-} + Fe^{3+}$$

When the concentration of hydrogen peroxide exceeds the concentration of iron(III), it is re-reduced by superoxide which is formed in a reaction of the $OH^{\bullet}$ radicals with hydrogen peroxide and the hydroxyl radical formation is

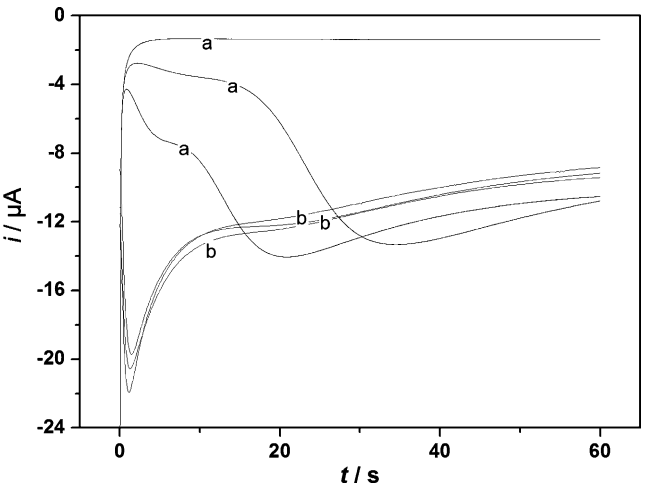

Fig. 2 Chronoamperometric curves of Pt deposition on two differently polished *pc*–Au electrodes: deposition potential E_{dep}=270 mV vs. Ag/AgCl, solution composition: 1×10^{-2} mol L^{-1} H_2PtCl_4 and 0.1 mol L^{-1} H_2SO_4. Curves measured with *pc*–Au electrodes following a "fine polish" are labeled by a, and curves measured with *pc*–Au electrodes following a "coarse polish" are labeled by b

continuing on account of the formed iron(II) until all hydrogen peroxide is consumed:

$$OH^{\bullet} + H_2O_2 \rightarrow H^+ + O_2^{-\bullet} + H_2O \text{ and } O_2^{-\bullet} + Fe^{3+} \rightarrow O_2 + Fe^{2+}$$

This reaction sequence can be formulated as the so-called iron-catalyzed Haber–Weiss reaction [21, 22]:

$$O_2^{-\bullet} + H_2O_2 \rightarrow O_2 + OH^{\bullet} + OH^-$$

Upon attack of the mechanically polished gold electrodes by hydroxyl radicals, the first nucleation peak is decreased. The current maxima decreased from about −21 μA to about −16 μA, which equals to a loss of 24% of active sites (Fig. 3). Very interestingly, and most probably nor by accident, this figure is near to the decrease of the real surface area by 30–37% found in earlier studies [6]. The decrease in the current of the first nucleation peak indicates a knockout of nucleation centers for the electrochemical deposition of platinum on gold. There is also a time shift of the maxima. However, the follow-up deposition at the second peak remains unaffected. The same experiments were performed with gold after the "fine polish" (Fig. 4a). Each line represents a freshly prepared electrode. The electrochemical deposition on the "fine polished" electrodes is highly irreproducible and the current transients vary considerably. However, the total charge of platinum reduction after treatment with hydroxyl radicals is certainly diminished; therefore, the deposited amount of platinum is decreased. The blocking effect of the hydroxyl radicals on the deposition of platinum on gold is clearly

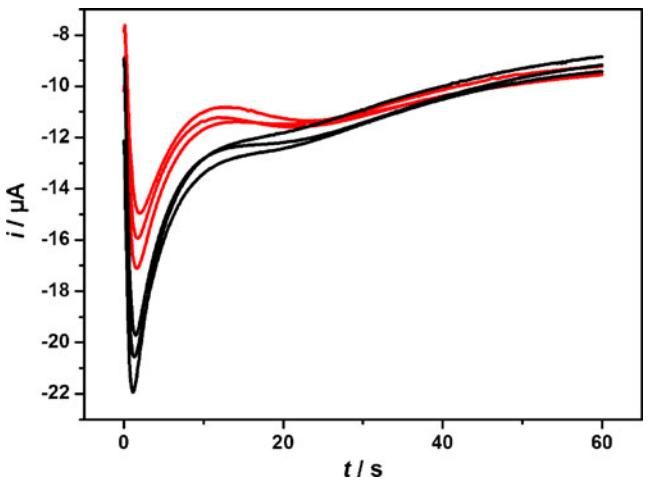

Fig. 3 Chronoamperometric curves of Pt deposition on *pc*–Au electrodes (after "coarse polish"): *red curves* are measured after a treatment of the electrodes with $OH^{\bullet}$ radicals, i.e., exposure to freshly prepared Fenton solutions (12 times, 5 min=1 h). The *black curves* were measured with untreated *pc*–Au electrodes. Deposition potential E_{dep}=270 mV vs. Ag/AgCl, solution composition: 1×10^{-2} mol L^{-1} H_2PtCl_4 and 0.1 mol L^{-1} H_2SO_4

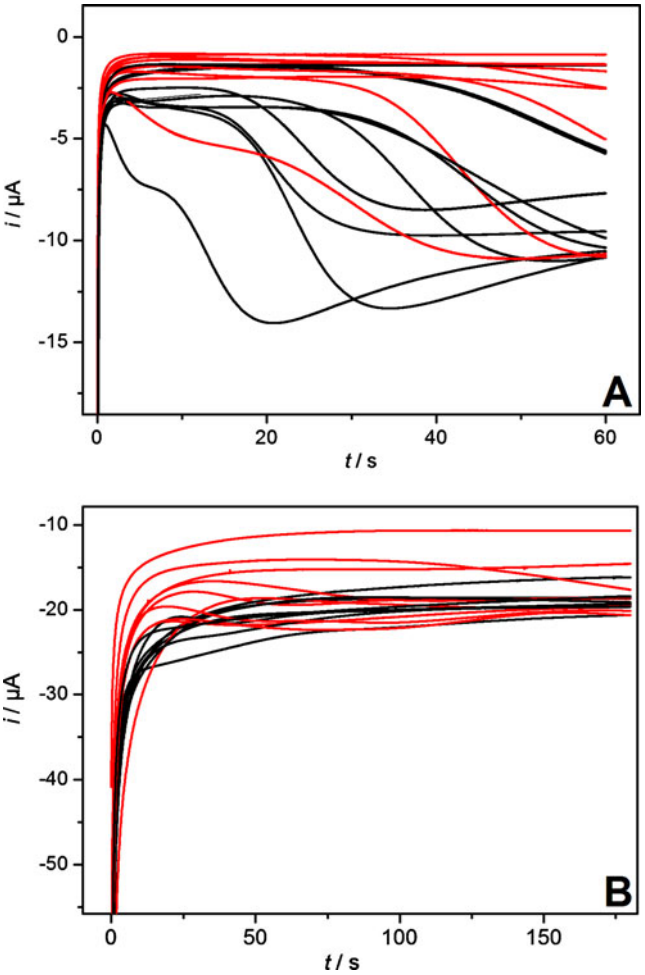

Fig. 4 Chronoamperometric traces of Pt deposition at E_{dep}=300 mV vs. Ag/AgCl from a solution containing **A** 1×10^{-2} mol L^{-1} K_2PtCl_4 and 0.1 mol L^{-1} H_2SO_4, and **B** 1×10^{-2} mol L^{-1} K_2PtCl_6 and 0.1 mol L^{-1} H_2SO_4. *Black lines* polycrystalline gold electrodes after "fine polish"; *red lines* polycrystalline gold electrodes after "fine polish" and following treatment with $OH^{\bullet}$ radicals for 1 h

visible. Nevertheless, the reproducibility is not as good as by using the "coarse polish": by measuring the effect of hydroxyl radicals on gold with H_2PtCl_6, the effect is not as big as with the bivalent platinum (Fig. 4b). Taking into account that Pt^{4+} exhibits deposition features of the Frank–van der Meerwe mode with the layer-by-layer growth and that the current is overlapping with the Cottrell behaving current due to the reduction of Pt^{4+} to Pt^{2+}, this supports our interpretation that $OH^{\bullet}$ radicals diminish the number of active sites.

After deposition, the relative amount of active platinum on gold can be estimated by cyclic voltammetry (Fig. 5) as follows: the peak between 0.3 and 0.4 V represents the reduction of the "Pt oxide" (or oxygen desorption from Pt, as others call it) and the peak between 0.8 and 0.9 V the reduction of "Au oxide" (or oxygen desorption from Au).

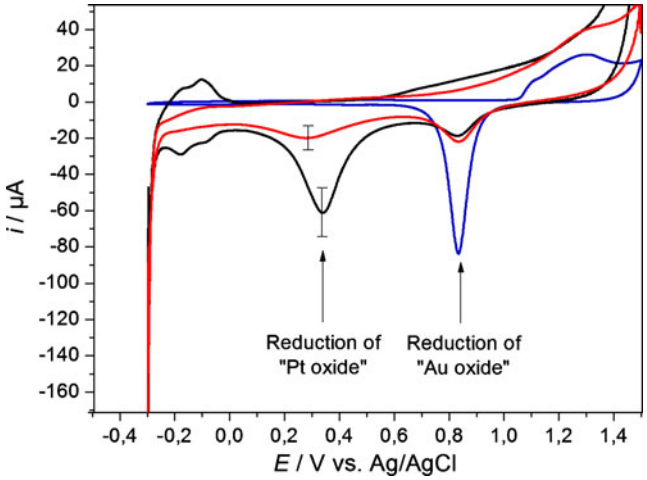

Fig. 5 Cyclic voltammograms (v=100 mV s^{-1}) in 0.1 mol L^{-1} H_2SO_4 solutions. *Blue curve* pristine gold electrode after "coarse polish". *Black curve* gold electrode ("coarse polish") after Pt deposition at E_{dep}=270 mV vs. Ag/AgCl in a solution containing 1×10^{-2} mol L^{-1} K_2PtCl_4 and 0.1 mol L^{-1} H_2SO_4 for 60 s. *Red curve* gold electrode ("coarse polish") treated for 1 h (12 times, 5 min) with freshly prepared Fenton solutions and recorded after Pt deposition (parameters like in case of *black curve*)

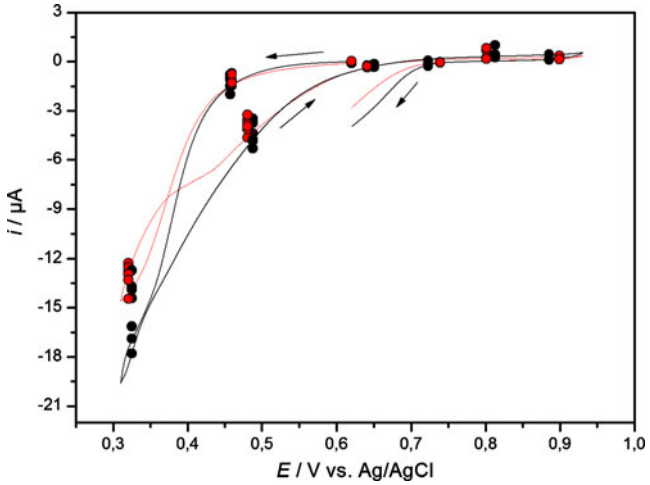

Fig. 6 *Black curves* first cycle of Pt deposition on pristine *pc*–Au electrodes (after "fine polish"); *red curve* first cycle of Pt deposition on *pc*–Au electrodes after "fine polish" and Fenton treatment for 1 h (12 times, 5 min). The *black* and *red dots* show the currents of repeated Pt depositions, as the depiction of the full curves would be confusing. Pt deposition was performed at a scan rate of 1 mV s^{-1} from solutions containing 1×10^{-2} mol L^{-1} H_2PtCl_6 and 0.1 mol L^{-1} sulphuric acid. Start potential, 0.62 V; starting direction, to negative potentials

To estimate the surface coverage of Au by Pt, the assumption was made that the charges underneath these peaks are proportional to the exposed metal surfaces. This assumption is certainly not exactly true, as the kinetics and potential dependence of formation and reduction of the two metal oxides, and also their structures certainly differ. However, to make a rough estimate of the relative surface areas, that assumption may be allowed. It is obvious from Fig. 5 that the amount of active platinum on the surface is less when the gold surface has been treated with hydroxyl radicals before deposition. The average ratio (q_{Pt} : q_{Au}) of 10 measurements for deposition of Pt on pristine *pc*–Au was 3.5, whereas for Fenton-treated *pc*–Au, the ratio dropped to 1.4.

The effect of a pretreatment of the gold electrode with Fenton solutions is also visible in the cyclic voltammograms depicted in Fig. 6 where Pt was deposited from H_2PtCl_6 solutions. The currents at E=0.33 V vary between −13 and −18 µA for the mechanically polished *pc*–Au and between −12 and −15 µA for Fenton polished *pc*–Au. The forward scan is crossing the backward scan, indicating a nucleation process. The onset potential, i.e., the potential where the reaction starts, is about 0.35 V vs. Ag/AgCl. The same experiments (not shown) were performed with K_2PtCl_4: the onset potentials were slightly moved to negative potentials and the currents at 0.3 V vs. Ag/AgCl were decreased; however, no significant difference between mechanically and Fenton polished *pc*–Au was observed. The cathodic current which builds up at potentials of 0.6–0.7 V with increasing Pt deposited on Au is due to the decreased overpotential of Pt deposition.

The kinetics of nucleation and growth of Pt on *pc*–Au electrodes was also analyzed in the formal framework of the Scharifker and Hill [23] approach. Scharifker and Hill have solved the Avrami theorem for multiple nucleations with growing diffusion zones. Two cases were distinguished, instantaneous and progressive growth. The instantaneous nucleation takes place at a constant number of active sites, whereas in the case of progressive nucleation the new phase nucleates, grows and the diffusion zones overlap during the entire period of observation. In case of three-dimensional (3-D) instantaneous nucleation, the following equation holds:

$$\left(\frac{i}{i_m}\right)^2 = \frac{1.9542}{\frac{t}{t_m}}\left\{1-\exp\left[-1.2564\left(\frac{t}{t_m}\right)\right]\right\}^2 \qquad (1)$$

and for 3-D progressive nucleation:

$$\left(\frac{i}{i_m}\right)^2 = \frac{1.2254}{\frac{t}{t_m}}\left\{1-\exp\left[-2.3367\left(\frac{t}{t_m}\right)^2\right]\right\}^2 \qquad (2)$$

Figure 7 depicts plots of the experimental results in the coordinates $(i/i_m)^2$ versus t/t_m and also the theoretical curves according to Eq. 1 (3-D instantaneous nucleation) and Eq. 2 (3-D progressive nucleation). Obviously, the nucleation follows the 3-D instantaneous mode. Further, the Fenton treatment does not change the nucleation mode. Waibel et al. [12] have mentioned that they observed 3-D progressive nucleation for the deposition of Pt on Au (100) and (111) single crystal surfaces.

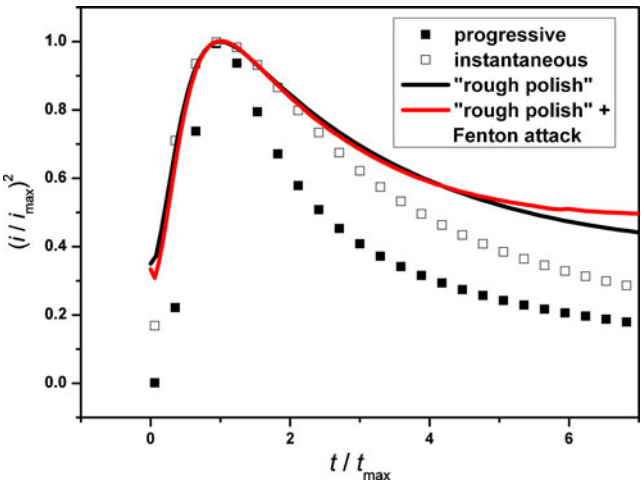

Fig. 7 Plots of Eq. 1 (3-D instantaneous nucleation; *white square*), Eq. 2 (3-D progressive nucleation; *black square*), and of the experimental results of Pt deposition transients using a pristine gold electrode after "coarse polish" (*black line*), and using a gold electrode which—after the "coarse polish"—has been treated with Fenton solutions for 1 h (12 times á 5 min; *red line*). The experimental data relate to the transients shown in Fig. 3

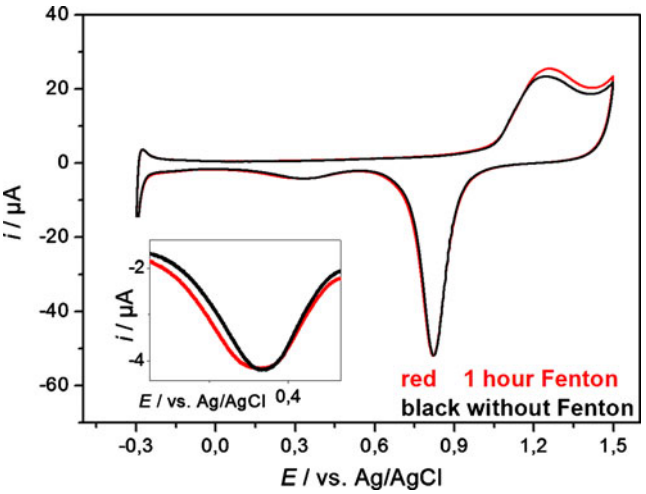

Fig. 8 Cyclic voltammograms recorded after spontaneous deposition of Pt on a pristine gold electrode after a "coarse polish" (*black curve*) and on a gold electrode which has been subjected to a Fenton treatment (1 h, i.e., 12 times, 5 min) after the "coarse polish" (*red curve*). The spontaneous deposition of Pt was carried out in solutions containing 3×10^{-3} mol L^{-1} H_2PtCl_4 and 0.1 mol L^{-1} H_2SO_4. The cyclic voltammograms were recorded in sulphuric acid (0.1 mol L^{-1} H_2SO_4) with scan rate v=50 mV s^{-1}

The effect of treating the pc–Au surface with hydroxyl radicals on the spontaneous nucleation of Pt on pc–Au

As mentioned in the "Introduction" section, Pt can be spontaneously deposited (without external application of a potential) on Au electrodes [15–17]. The detailed mechanism of this deposition is still debated [17]; however, it is very likely that a strong adsorption of $[PtCl_4]^{2-}$, as it is known to occur [16], plays a role. We wanted to see if that spontaneous deposition will be affected by a treatment of the *pc*–Au electrodes with hydroxyl radicals. Figure 8 shows that the spontaneous Pt deposition is practically not affected by the Fenton treatment. These results can be taken as indication that the active sites for the spontaneous Pt deposition differ from those for the electrochemical deposition. From the work of Nagahara et al., it is clear that the adsorption of $[PtCl_4]^{2-}$ occurs on regular surface sites and not at specific active sites in the sense of surface defects. Hence, it is understandable that the treatment of the *pc*–Au surface which is known to affect only active sites (surface defects) [6, 7] is not affecting the spontaneous Pt deposition.

In situ atomic force microscopy of electrochemical deposition of Pt on pc–Au

In further experiments, the nucleation and growth of Pt on Au was studied by in situ AFM. For that purpose, a home-made electrochemical cell (Fig. 9) was placed under the atomic force microscope so that the topography of the *pc*–Au disk electrode could be imaged. The AFM was used in the contact mode. Figure 10a shows an atomic micrograph of the *pc*–Au electrode after the "fine polish" recorded at 620 mV (i.e., the standby potential where no Pt deposition takes place) in a solution containing 0.1 mol L^{-1} sulphuric acid and 5×10^{-3} mol L^{-1} K_2PtCl_4. In order to reduce the deposition time to values below 1 s for minimizing time shifts of the images, the deposition was performed at

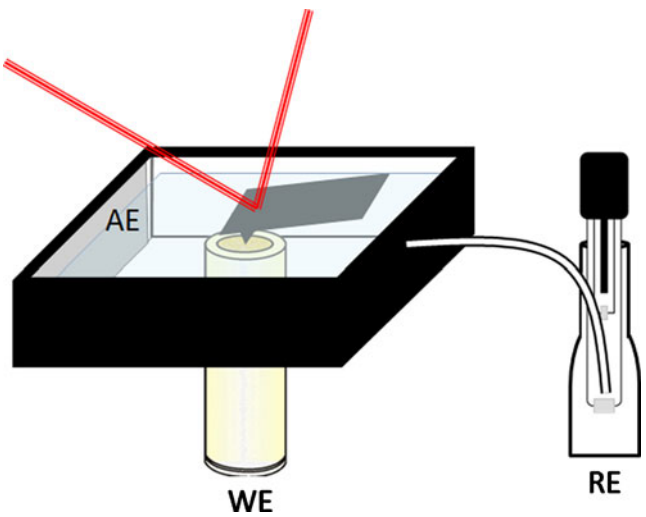

Fig. 9 Home-made electrochemical cell with a polycrystalline gold disk as the working electrode (WE), a platinum auxiliary electrode (AE), and an Ag/AgCl (3 mol L^{-1} KCl) reference electrode (RE) which was connected with a polyethylene tube filled with KCl saturated agar gel. The cell was placed directly under the atomic force microscope

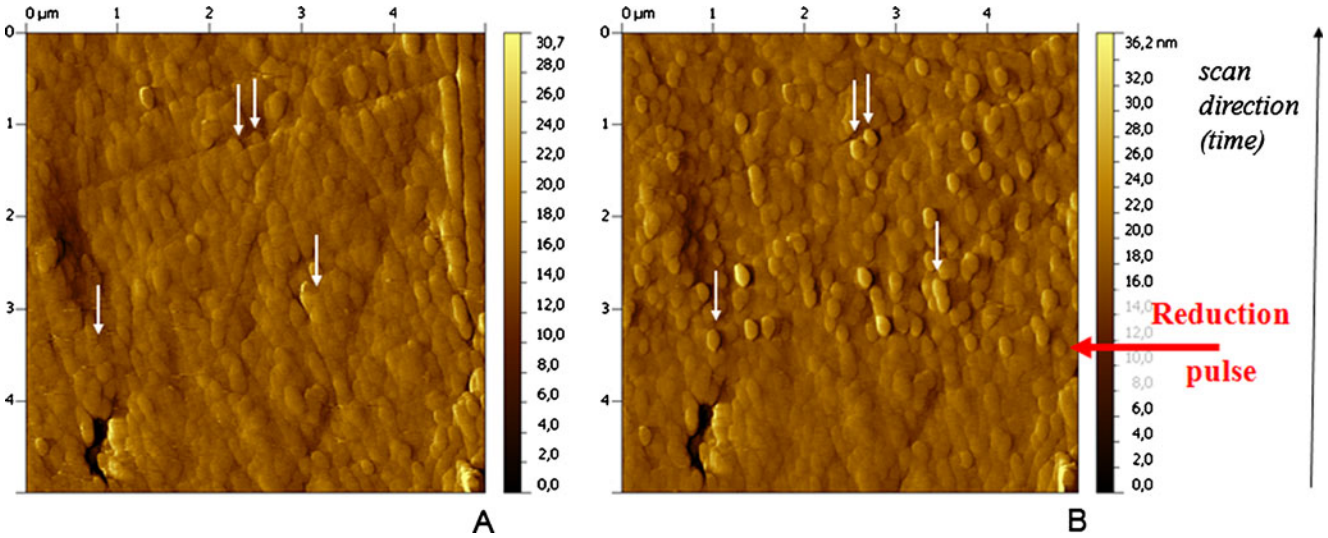

Fig. 10 AFM micrograph of bulk deposition of platinum on a *pc*–Au electrode. Electrochemical deposition was followed in situ with an atomic force microscope in deflection mode in a solution containing 0.1 mol L^{-1} H_2SO_4 and 5×10^{-3} mol L^{-1} K_2PtCl_4. **A** Gold substrate, **B** gold substrate during deposition (deposition was started potentiostatically at E_{dep}=−300 mV vs. Ag/AgCl for 0.8 s so that the pulse was applied when the micrograph recording reached the stage indicated by the *red arrow*)

−300 mV. Already after a very short pulse deposition of Pt (pulse time t_p=0.8 s, pulse potential t_p=−300 mV), one can observe that certain gold grains grew (see the marks in Fig. 10a and b) whereas other grains remained unchanged. The electrode surface is getting rougher during the deposition (at least in the first stages of deposition). This can be also deduced from profiles (Fig. 11) which have been measured for Pt deposition at +300 mV, i.e., exactly at the same potential as in case of the purely electrochemical studies: the profile (cut) shows that some grains grew and others remained unchanged. For these profiles, the AFM images were recorded using a much more diluted K_2PtCl_4 solution (1×10^{-4} mol L^{-1}) and a longer deposition pulse duration (t_p=20 s). This behavior can be explained as follows: some gold grains are active towards the nucleation of Pt and these active sites prompt the growing of Pt on these gold grains so that these gold grains are decorated by a Pt layer.

In further experiments, the effect of $OH^{\bullet}$ radicals on Pt deposition was also studied by in situ AFM. Figure 12 shows in situ atomic force micrographs analogous to those shown in Fig. 10, but using a *pc*–Au electrode which has been treated with $OH^{\bullet}$ radicals generated in the UV reactor. Like in the case of Fig. 12, it can be seen that only certain Au grains are covered by Pt. No obvious differences between an untreated and an $OH^{\bullet}$-treated electrode could be observed. This is not surprising because the electrochemical experiments have shown only differences in the absolute amounts of deposited Pt, a feature which cannot be easily deduced from the atomic force micrographs.

Conclusions

The results of this study can be summarized as follows:

1. The electrochemical nucleation and growth of Pt on polycrystalline Au electrodes is much more reproducible when the electrodes underwent a mechanical “coarse polish” compared to a mechanical “fine polish”.
2. Treatment of the polycrystalline Au electrodes with $OH^{\bullet}$ radicals diminishes the number of active sites on the Au surface. Quantitatively, this diminishing (24%) is at the same order of magnitude as the diminishing of real electrode surface area (30–37%) found in a previous study. Although it cannot be excluded that the decrease of the number of active sites is the effect of decreased real surface area, we advocate the view that it is a real knockout of active sites, very much as in case of the knockout of electrocatalytic sites reported previously [7]. The unaffected spontaneous Pt deposition further supports that view.
3. The electrochemical deposition of Pt on polycrystalline Au electrodes follows a 3-D instantaneous nucleation, both for Au electrodes *before* and *after* treatment with $OH^{\bullet}$ radicals.
4. The spontaneous deposition of Pt on polycrystalline Au is unaffected by $OH^{\bullet}$ radicals.
5. In situ AFM experiments show that the Pt grows on top of some of the Au grains, apparently on those which have active sites on their surface. This leads to a roughening of the electrode surface upon Pt deposition.

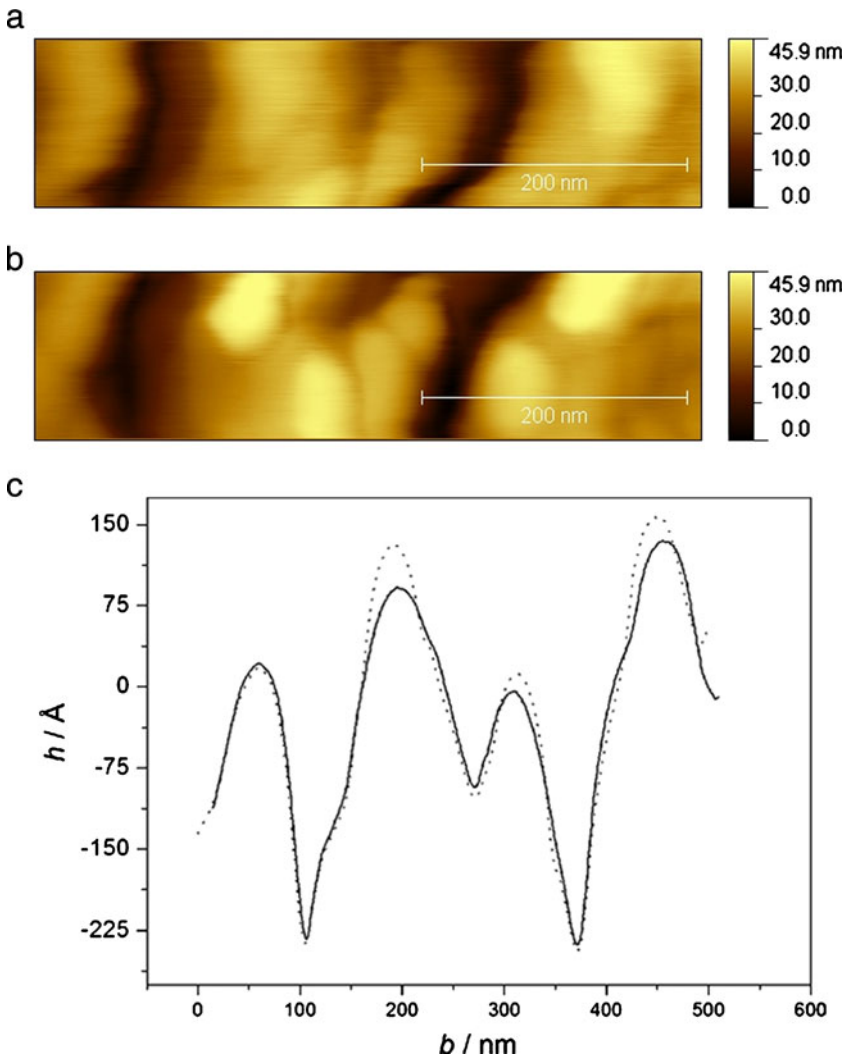

Fig. 11 First deposition stage of platinum on polycrystalline gold. **a** Atomic force micrograph of the pristine *pc*–Au electrode ("fine polish") before Pt deposition. **b** Atomic force micrograph of the same area shown in **a**; however, after Pt deposition from a solution containing 1×10^{-4} mol L^{-1} H_2PtCl_4 and 0.1 mol L^{-1} H_2SO_4 applying a deposition pulse of 20 s at E_{dep}=300 mV vs. Ag/AgCl. **c** Profiles of a cut through the images **a** (*full line*) and **b** (*dotted line*)

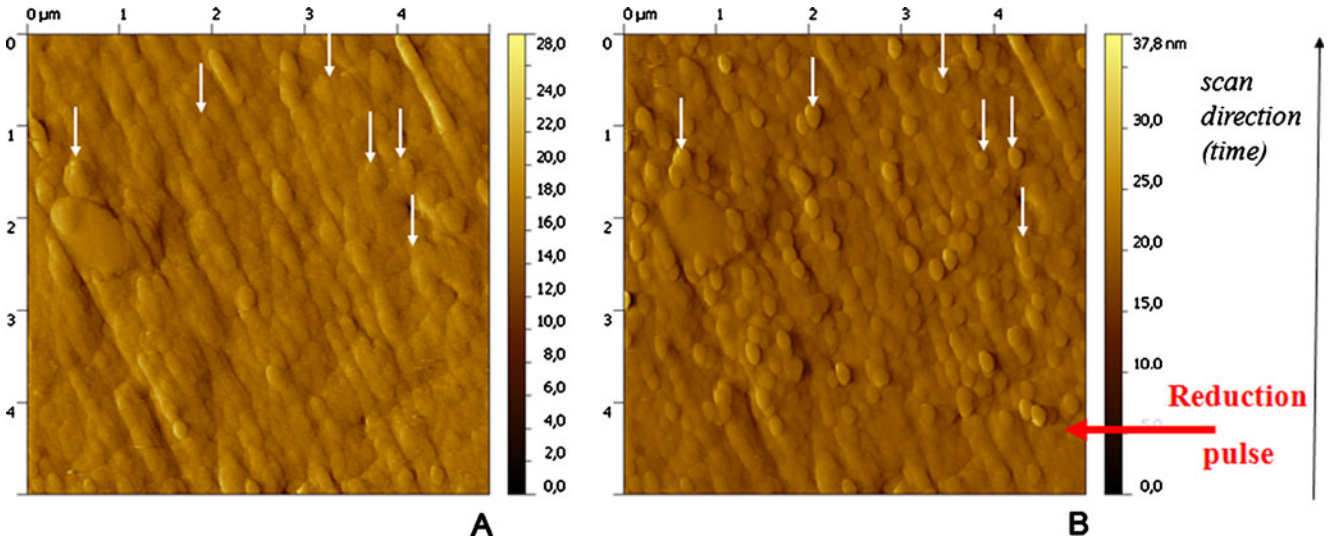

Fig. 12 In situ AFM micrograph of bulk deposition of platinum on a *pc*–Au electrode treated in the UV Reactor for 5 min in defelection mode. Electrochemical deposition was followed in situ with an atomic force microscope in solution containing 0.1 mol L^{-1} sulphuric acid with 5×10^{-3} mol L^{-1} K_2PtCl_4. **A** Gold substrate before deposition, **B** gold substrate during deposition: the deposition was started potentiostatically at E_{dep}=–300 mV vs. Ag/AgCl for 0.8 s so that the pulse was applied when the micrograph recording reached the stage indicated by the *red arrow*

The results allow the following interpretation:

1. The higher reproducibility of deposition experiments with the mechanical "coarse polish" electrodes is probably the result of a much larger number of active sites, and thus *better averaging* of the quality and quantity of the active sites.
2. The diminishing of the number of active sites without indication of a change of the quality of active sites can be seen as the result of a chemical knockout of the active sites, very similar to the knockout of the electrocatalytic sites observed earlier.
3. The phenomenon that the $OH^{\bullet}$ treatment does not change the nucleation mode in electrochemical deposition experiments (always 3-D instantaneous nucleation) also indicates that the active sites are not qualitatively altered.
4. The result that the spontaneous Pt deposition on *pc*–Au, i.e., deposition without application of an external potential, is not only qualitatively, but also quantitatively unaffected by the $OH^{\bullet}$ radicals, indicates that the active sites for that deposition reaction are not the same as those for the electrochemical deposition. Most probably, and in agreement with recent findings [17], the spontaneous deposition is based on an isotropic adsorption of Pt ions on the Au surface.
5. The in situ AFM experiments can be interpreted both on the basis of a Volmer–Weber and a Stranski–Krastanov mechanism. In view of the findings of Mathur and Erlebacher [14], the latter mechanism may seem likely; however, the fact that the number of Pt nuclei is diminished after treatment of the *pc*–Au with $OH^{\bullet}$ radicals indicates that a monolayer underneath the growing Pt crystals is unlikely. The idea of a Pt monolayer is not compatible with the idea of specific active sites on Au.
6. The results do not contradict the hypothesis that the active centers for electrocatalysis of oxygen reduction and for Pt deposition may be indeed the same. The partially filled d-orbitals of Au atoms, which are supposed to be the active sites of oxygen reduction [7], can easily be the active sites of the deposition of the first Pt atoms with the formation of Au–Pt bonds. This nucleation scenario would be in agreement with the recently proposed chemical model of nucleation, which is based on the assumption that the active site is active because it possesses the ability to form a strong chemical bond with the nucleating species [24].
7. The results shine new light on earlier models of active sites of gold electrodes propagated by Burke et al. [25–28]. Indeed, the active sites are obviously highly reactive gold species on the gold surface.
8. The results also allow a better understanding of the activity of gold implants: Danscher [29] and Danscher and Larsen [30] have shown that gold ions are liberated from gold implants, and that is now, on the basis of our studies, understandable as dissolution of active gold sites by free oxygen radicals which are typically formed in immune defense reactions.

From that summary and the interpretation, the following future tasks can be derived:

– It is necessary to study the effect of $OH^{\bullet}$ radicals on the deposition of Pt on single crystal gold electrodes using scanning tunneling microscopy and AFM.
– It would be highly interesting to perform experiments revealing the spatial distribution of electrocatalytic centers (e.g., for oxygen reduction) and to compare these activity maps with the activity maps for Pt deposition. Only such experiments may provide the answer to the most crucial question: are the active centers for electrocatalysis of oxygen reduction identical with the active centers of Pt deposition (or any other electrocatalytic and deposition reactions) and what is their real nature?

Acknowledgment Gustav Sievers was supported by a fellowship of the Alfried Krupp Wissenschaftskolleg Greifswald. The authors acknowledge extensive experimental support by Oliver Nehrlich.

References

1. Zambelli T, Wintterlin J, Trost J, Ertl G (1996) Identification of the "Active Sites" of a surface-catalyzed reaction. Science 273:1688–1690
2. Taylor HS (1925) A theory of the catalytic surface. Proc R Soc A 108:105–111
3. Thomas JM (2006) The tortuous tale of the catalytically active site. Top Catal 38:3–5
4. Budevski E (2000) Electrocrystallization nucleation and growth phenomena. Electrochim Acta 45:2559–2574
5. Christensen CH, Nørskov JK (2008) A molecular view of heterogeneous catalysis. J Chem Phys 128:182503
6. Nowicka AM, Hasse U, Hermes M, Scholz F (2010) Hydroxyl radicals attack metallic gold. Angew Chem Int Ed 49:1061–1063
7. Nowicka AM, Hasse U, Sievers G, Donten M, Stojek Z, Scholz F (2010) Selective knock-out of gold active sites. Angew Chem Int Ed 49:3006–3009
8. Rapecki T, Nowicka AM, Donten M, Scholz F, Stojek Z (2010) Activity changes of glassy carbon electrodes caused by their exposure to OH• radicals. Electrochem Commun 12:1531–1534
9. Nowicka AM, Hasse U, Donten M, Hermes M, Stojek Z, Scholz F (2011) The treatment of Ag, Pd, Au and Pt electrodes with OH radicals reveals information on the nature of the electrocatalytic centres. J Solid State Electrochem 15:2141–2147
10. Rodriguez JA, Goodman DW (1995) Chemical and electronic properties of bimetallic surfaces. Acc Chem Res 28:477–478

11. Chen M, Goodman D (2004) The structure of catalytically active gold on titania. Science 306:252–255
12. Waibel H, Kleinert ML, Kibler LA, Kolb DM (2002) Initial stages of Pt deposition on Au(111) and Au(100). Electrochim Acta 47:1461–1467
13. Kondo T, Shibata M, Hayashi N, Fukumitsu H, Masuda T, Takakusagi S, Uosaki K (2010) Resonance surface X-ray scattering technique to determine the structure of electrodeposited Pt ultrathin layers on Au(111) surface. Electrochim Acta 55:8302–8306
14. Mathur A, Erlebacher J (2008) Effects of substrate shape, curvature and roughness on thin heteroepitaxial films of Pt on Au(111). Surf Sci 602:2863–2875
15. Strbac S, Petrovic S, Vasilic R, Kovac J, Zalar A, Rakocevic Z (2007) Carbon monoxide oxidation on Au(111) surface decorated by spontaneously deposited Pt. Electrochim Acta 53:998–1005
16. Nagahara Y, Hara M, Yoshimoto S, Inukai J, Yau SL, Itaya K (2004) In situ scanning tunneling microscopy examination of molecular adlayers of haloplatinate complexes and electrochemically produced platinum nanoparticles on Au(111). J Phys Chem B 108:3224–3230
17. Bakos I, Szabó S, Pajkossy T (2011) Deposition of monoatomic platinum layers on gold. J Solid State Electrochem. doi:10.1007/s10008-011-1444-2
18. Bostanov V, Obretenov W, Staikov G, Roe DK, Budevski E (1981) J Crystal Growth 52(1981):761–765
19. Fenton HJH (1894) LXXIII—Oxidation of tartaric acid in presence of iron. J Chem Soc Trans 65:899–910
20. Halliwell B, Gutteridge J (2007) Free radicals in biology and medicine. Oxford University Press, Oxford, UK
21. Liochev SI, Fridovich I (2002) The Haber–Weiss cycle—70 years later: an alternative view. Redox Rep 7:55
22. Haber F, Weiss J (1934) The catalytic decomposition of hydrogen peroxide by iron salts. Proc R Soc A 147:332–351
23. Scharifker B, Hills G (1983) Theoretical and experimental studies of multiple nucleation. Electrochim Acta 28:879–889
24. Scholz F (2011) Active sites of heterogeneous nucleation understood as chemical reaction sites. Electrochem Commun 13:932–933
25. Burke LD, O'Mullane AP (2000) Generation of active surface sites of gold and the role of such states in electrocatalysis. J Solid State Electrochem 4:285–297
26. Burke LD, Hurley LM (2002) An investigation of the electrochemical responses of superactivated gold electrodes in alkaline solutions. J Solid State Electrochem 6:101–110
27. Burke LD, Moran JM, Nugent PF (2003) Cyclic voltammetry responses of metastable gold electrodes in aqueous media. J Solid State Electrochem 7:529–538
28. Burke LD (2004) Scope for new applications for gold arising from the electrocatalytic behaviour of its metastable surface states. Gold Bull 37:125–135
29. Danscher G (2002) In vivo liberation of gold ions from gold implants. Autometallographic tracing of gold in cells adjacent to metallic gold. Histochem Cell Biol 117:447–452
30. Danscher G, Larsen A (2010) Effects of dissolucytotic gold ions on recovering brain lesions. Histochem Cell Biol 133:367–373
31. Matthews JW, Jesser WA (1967) Experimental evidence for pseudomorphic growth of platinum on gold. Acta Met Mater 15:595–600
32. Sachtler J, Van Hove M, Biberian J, Somorjai G (1981) The structure of epitaxially grown metal films on single crystal surfaces of other metals: Gold on Pt (100) and platinum on Au (100). Surf Sci 110:19–42
33. Sugawara A, Nittono O (1991) Interface structures of Pt/Au(001) epitaxial bilayer films prepared by means of ion beam sputtering. J Crystal Growth 115:596–601
34. Friedrich K, Marmann A, Stimming U, Unkauf W, Vogel R (1997) Model electrodes with defined mesoscopic structure. Fresenius J Anal Chem 358:163–165